CHEMISTRY OF MATERIALS

pubs.acs.org/cm

Article

Rational Design of Efficient Heavy-Atom-Free Boron-Dipyrromethene Nanophotosensitizers for Two-Photon Excited Photodynamic Therapy of Cancer

Van-Nghia Nguyen,[⊥] Dong Joon Lee,[⊥] Dianqi Zhang,[⊥] Jeongsun Ha,[⊥] Kunemadihalli Mathada Kotraiah Swamy, Rui Wang,* Hwan Myung Kim,* Fabiao Yu,* and Juyoung Yoon*

Cite This: *Chem. Mater.* 2024, 36, 5534−5541

Read Online

ACCESS | Metrics & More | Article Recommendations | Supporting Information

ABSTRACT: Although boron-dipyrromethene (BODIPY) dyes have been widely recognized for their potential use as photosensitizers (PSs) in cancer treatment, the development of heavy-atom-free BODIPY PSs for photodynamic therapy (PDT), particularly in two-photon excited photodynamic therapy (2PE−PDT), remains challenging. Herein, a novel heavy-atom-free photosensitizer (BDP-6) with optimized singlet−triplet energy gap and steric hindrance was designed and synthesized to facilitate intersystem crossing and improve fluorescence intensity. To enhance the biocompatibility and tumor-targeting ability of BDP-6, corresponding nanophotosensitizers (BDP-6 NPs) were prepared by encapsulating BDP-6 within DSPE-PEG(2000) biotin. Compared to control BDP-5 NPs without dimethyl groups, BDP-6 NPs exhibited brighter deep red fluorescence and higher efficiency in generating reactive oxygen species (ROS) under one-photon excitation in aqueous solutions. Moreover, BDP-6 NPs displayed excellent tumor-targeting ability, bright red emission, and considerable phototoxicity with low dark toxicity toward cancer cells. Notably, under two-photon excitation, the BDP-6 NPs efficiently generated ROS both in aqueous solutions and living cells, thereby demonstrating exceptional performance in 2PE−PDT for cancer cell ablation. Furthermore, in vivo experiments revealed that BDP-6 NPs hold great promise for cancer PDT. Our work presents practical strategies for developing tumor-targeting heavy-atom-free nanophotosensitizers based on BODIPY dye for 2PE−PDT of cancer.

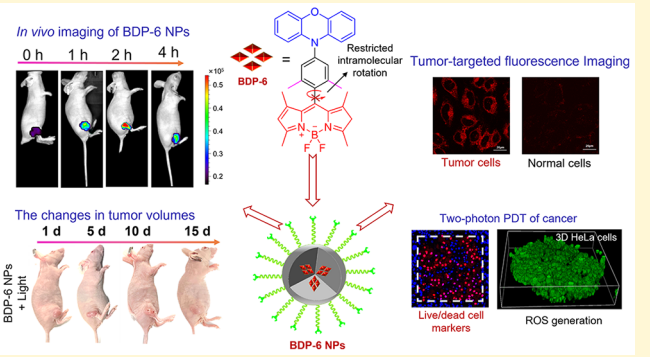

1. INTRODUCTION

Photodynamic therapy (PDT) has great potential for treating cancer and other diseases due to its distinguished advantages over traditional therapies.[1−5] The key element in this treatment is the photosensitizer (PS), which results in therapeutic outcomes from reactive oxygen species (ROS) production with light irradiation in the presence of oxygen.[6−8] Generally, PSs should be capable of simultaneous fluorescence imaging and treatment, which allows the real-time monitoring of tumors and reflecting the feedback of the therapeutic effects during the PDT.[9−12] So far, there are two strategies to achieve clinical PSs.[13] One relies on a molecular design approach to modulate the photophysical processes of PSs with the support of the Jablonski diagram. This is because the photophysical processes of PSs are highly associated with absorbed photon conversion into photodynamic effects, while simultaneously, various functional groups can be covalently conjugated through chemical reactions. This method, however, requires a complicated synthesis and is expensive.[14,15] The other strategy is a nanoengineering approach integrating multiple components into one nanoparticle. Nanoengineering is a convenient and effective approach, but numerous components, multistep fabrication, and low reagent loading hampers further clinical translation.[16] Although extensive studies have been conducted in both basic science and clinical applications, PDT for cancer cannot fully meet the requirement.

To treat deep-seated tumors, the excitation wavelength of PSs should be tuned to the phototherapeutic window (650−850 nm) because visible light is often quickly absorbed and scattered by biomolecules.[17] It is difficult to design and synthesize long-wavelength absorbing PSs with optimized

Received: February 21, 2024
Revised: May 14, 2024
Accepted: May 15, 2024
Published: May 23, 2024

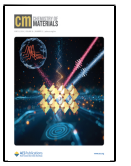

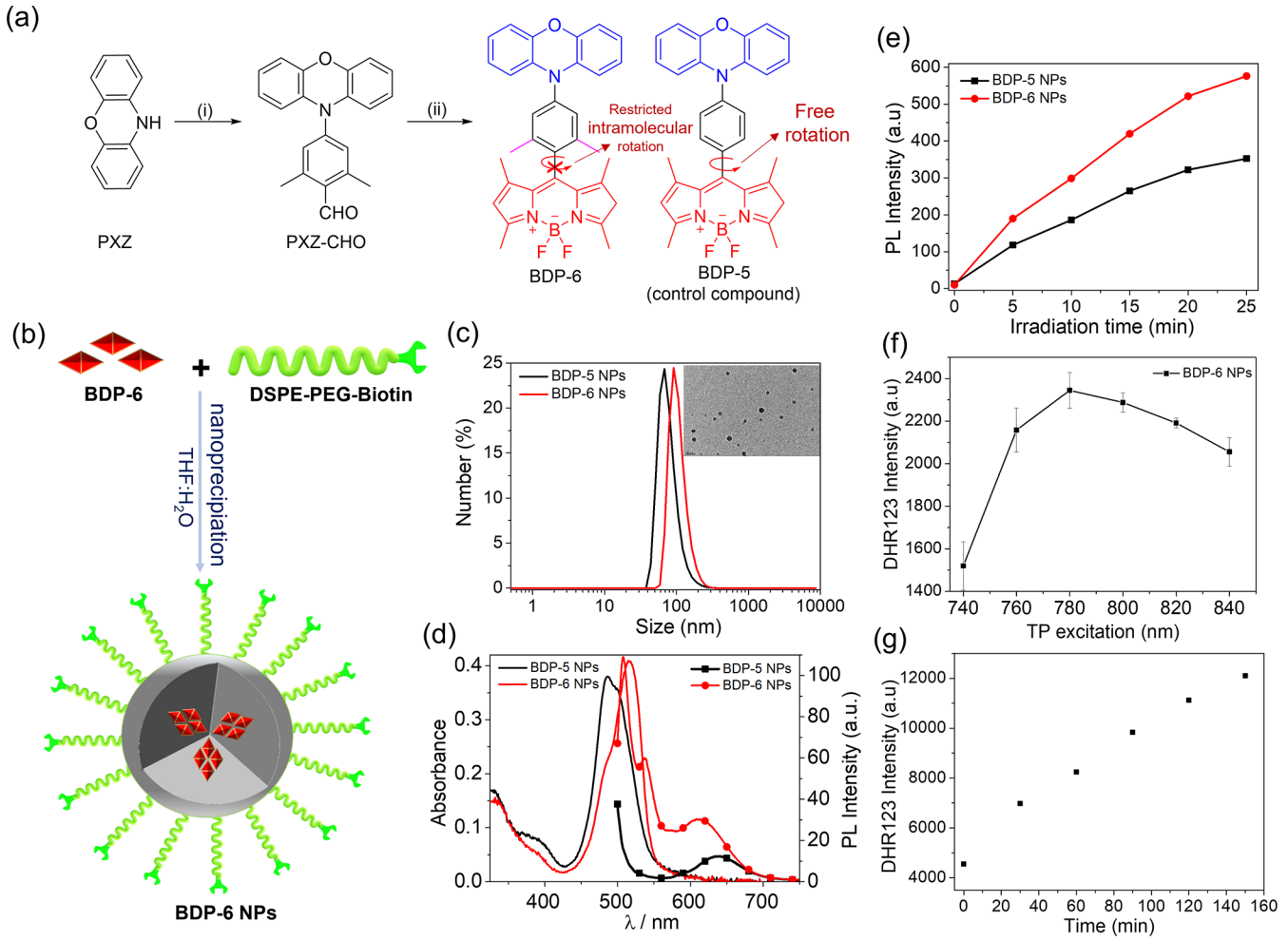

Figure 1. (a) Chemical structures and synthetic route of BDP dyes. (i) 4-bromo-2,6-dimethylbenzaldehyde, $Pd(OAc)_2$, *t*-Bu_3PHBF_4, and K_2CO_3, toluene, reflux. (ii) DMF, $POCl_3$. (iii) 2,4-dimethypyrrole, trifluoroacetic acid (TFA), *p*-chloranil, Et_3N, and $BF_3{\cdot}OEt_2$, CH_2Cl_2. (b) Schematic illustration for the preparation of BDP-6 NPs. (c) Nanoparticle size distribution of BDP PSs detected by DLS and TEM images (inset) of BDP-6 NPs. (d) UV−vis absorption and PL spectra of the BDP-5 NPs and BDP-6 NPs (10 μM, in water, λ_{ex} = 490 nm). (e) ROS generation of BDP-5 NPs and BDP-6 NPs in water after irradiation by a green LED (20 mW/cm^2) using DCFH-DA as ROS probe (λ_{ex} = 500 nm, λ_{em} = 525 nm). (f, g) Two-photon ROS generation efficiency of BDP-6 NPs (10 μM). (f) Plot of fluorescence intensity of DHR123 (2.5 μM) with BDP-6 NPs according to the two-photon excitation wavelength. (g) Plot of fluorescence intensity for DHR123 with BDP-6 NPs against TP irradiation time at 780 nm (λ_{ex} = 500 nm, λ_{em} = 525 nm).

triplet energy using one-photon excitation photodynamic therapy (1PE−PDT). Two-photon excitation photodynamic therapy (2PE−PDT) offers an opportunity to overcome light penetration and treatment depth issues.[3,18−22] The development of efficient two-photon PSs is promising for deep-seated tumor treatment.

Over the past decades, motivated by the inherent advantages of boron-dipyrromethene (BODIPY) dyes, such as excellent photophysical and photochemical properties, good photostability, and ease of modifications,[23−26] a large number of BODIPY-based PSs have been developed for oncologic PDT.[27−32] To overcome the shortcomings of BODIPY PSs containing heavy atoms, several BODIPY PSs without heavy atoms have been developed and studied in vivo.[33,34] However, examples of far-red/NIR BODIPY PSs for 2PE−PDT are rare.[35−37] Recently, we have provided a novel approach to efficient heavy-atom-free BODIPY PS by reducing the energy gap (ΔE_{ST}) between the lowest singlet (S_1) and lowest triplet excited states (T_1).[34] Introducing an electron donor to a BODIPY acceptor at *meso*-position via phenyl bridge significantly reduced ΔE_{ST}, resulting in a promoted intersystem crossing (ISC) process and enhanced ROS generation. We propose that tuning ΔE_{ST} along with blocking nonradiative decay pathways may further improve the ROS generation ability as well as the fluorescence quantum yields in restricted states. In addition, taking advantage of nanotechnology, nanophotosensitizers (NPSs) with good biocompatibility, high brightness, and excellent targeting capability can be afforded to enhance PDT.[38,39]

To validate this approach, we synthesized a novel heavy-atom-free BODIPY PS with a twisted D−A skeleton (BDP-6) to minimize ΔE_{ST} for efficient ISC and block intramolecular rotation for enhanced fluorescence intensity. BDP-6 NPs with deep red emission, high ROS generation ability, and high biocompatibility were further produced. BDP-6 NPs exhibited excellent tumor-targeting capability and considerable PDT performance with low dark cytotoxicity under green light irradiation. Remarkably, outstanding performance in 2PE−PDT for cancer cell ablation was observed for BDP-6 NPs under two-photon excitation. Furthermore, in vivo studies

https://doi.org/10.1021/acs.chemmater.4c00482
Chem. Mater. 2024, 36, 5534−5541

indicated that BDP-6 NPs displayed great promise for tumor-targeted fluorescence imaging and PDT. We believe this work will offer simple strategies to guide the design of tumor-targeting, two-photon, heavy-atom-free nanophotosensitizers based on BODIPY dye, thereby facilitating the development of PDT.

2. RESULTS AND DISCUSSION

2.1. Molecular Design, Preparation of Tumor-Targeting NPs, Photophysical Properties of NPs. Motivated by previous work, we designed and synthesized a heavy-atom-free BODIPY PS (BDP-6) for enhanced PDT of cancer in this study. Phenoxazine (PXZ) was introduced to the *meso*-position of the BODIPY acceptor via the phenyl linker, which contained two *ortho*-methyl groups, to block the rotational nonradiative decay channel further. PXZ was selected as the donor because of its strong electron-donating capability and steric bulkiness to tune ΔE_{ST}. This leads to an efficient ISC process. BDP-6 and BDP-5 (control compound) were obtained in good yields from two steps starting from phenoxazine, followed by a literature modification (Figure 1a).[34] BDP-6 was fully characterized using ^{1}H and ^{13}C NMR and high-resolution mass spectrometry (Figures S1 and S2). To realize the biomedical applications in physiological conditions, BDP-6 was encapsulated into 1,2-distearoyl-*sn*-glycero-3-phosphoethanolamine-*N*-[biotinyl-(poly(ethylene glycol))-2000] (DSPE-PEG(2000) biotin, an amphiphilic matrix) to produce biocompatible and tumor-targeting (passive and active targeting) BDP-6 NPs via nanoprecipitation method (Figure 1b). BDP-6 NPs were characterized by dynamic light scattering (DLS) with spherical morphology and an average size of ∼70 nm. This matched well with transmission electron microscopy (TEM) images (Figure 1c). As shown in Figure 1d, BDP-5 NPs and BDP-6 NPs exhibited similar absorption spectra with a strong absorption peak centered at 500 nm, as observed with other BODIPY dyes.[40] On the other hand, the fluorescence intensity of BDP-6 NPs with a maximum of 620 nm was much higher than that of BDP-5 NPs, indicating the important role of dimethyl groups in blocking BDP-6 intramolecular rotation in a restricted state. The BDP-6 NPs were also highly stable under photoexcitation (Figure S3).

Inspired by the remarkable fluorescence enhancement of BDP-6 in a restricted state, we evaluated the ROS generation capability of BDP-6 NPs in aqueous media under one-photon excitation (green LED, 20 mW/cm^2) using DCFH-DA as an indicator. The results demonstrated that BDP-6 NPs showed an approximately 1.6-fold higher ROS generation efficiency than BDP-5 NPs and a similar ROS generation efficiency to that of erythrosine B (a commonly used photosensitizer for studies in biological systems), suggesting that BDP-6 NPs were favorable candidates for TP-induced PDT (Figures 1e and S4a). To that end, the TP irradiation-triggered ROS generation of BDP-6 NPs was evaluated, where we irradiated a solution containing BDP-6 NPs and dihydrorhodamine 123 (DHR123 is oxidized to fluorescent rhodamine 123 by ROS) with TP in a 740−840 nm (10 nm intervals) wavelength range. Upon TP excitation at 100 mW power, we observed a sharp emission signal at 526 nm as an indication of rhodamine 123 formation. After 30 min at 100 mW power, DHR123 turn-on response was highest at 780 nm, and continuous TP exposure for 160 min showed gradual ROS generation (Figure 1f,g).

2.2. Cell Imaging and One-Photon Excited PDT In Vitro. In the preliminary biological study, we evaluated cell imaging capability by incubating BDP-6 NPs with HeLa cells (a cervical cancer cell line) and WI38 cells (a normal cell line), respectively. While the red fluorescence signal in HeLa cells with BDP-6 NPs was clearly observed, the confocal microscopy images showed negligible red fluorescence signals in WI38 cells, as illustrated in Figures 2a and S6, indicating the high specificity of BDP-6 NPS for cancer cells. This behavior could be attributed to the abnormal expression of biotin receptors in cancer cells.[41] An intracellular ROS production and a dead cell viability assay were also performed under green light excitation, as depicted in Figure 2b. It was also observed that green light irradiation did not cause cytotoxic effects in the absence of BDP-6 NPs. In sharp contrast, upon green light exposure, BDP-6 NPs displayed a low 0.35 μM half-maximal inhibitory concentration (IC50) (Figure 2c). These results demonstrated that BDP-6 NPs could efficiently target cancer cells and enhance the PDT effect.

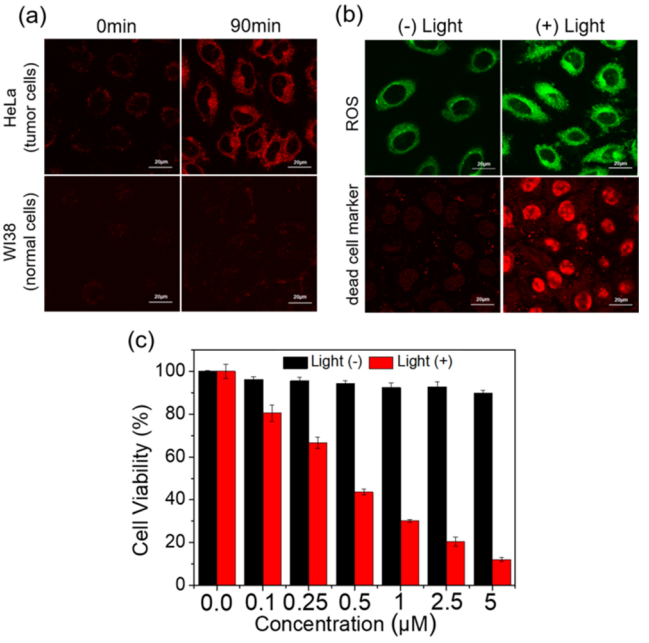

Figure 2. Fluorescence microscope images of (a) HeLa (cancer cells) and WI38 (normal cells) cells after treatment with BDP-6 NPs (5 μM) and (b) loaded with DCFH-DA (total ROS probe) or PI (4 μM, dead cell marker). (c) Cell viability of HeLa cells after treatment with different concentrations of BDP-6 NPs with green light irradiation.

2.3. Two-Photon Excited PDT In Vitro. To investigate the intracellular ROS generation of the BDP-6 NPs under TP excitation, we stained HeLa cells with DCFH-DA (ROS indicator) without BDP-6 NPs for 30 min and irradiated a section with 780 nm TP light. The DCFH-DA fluorescence did not increase, even with increased TP scans, indicating insufficient ROS-mediated DCF formation. After 30 min without DCFH-DA, constant fluorescence with TP irradiation on BDP-6 NP-stained HeLa cells showed BDP-6 NPs distributed in the cytoplasm. This also illustrated that BDP-6 NPs were highly photostable under TP-induced PDT conditions (Figure S9). However, when the HeLa cells were stained with DCFH-DA and BDP-6 NPs, the green fluorescence of DCFH-DA was observed, and DCF intensity was further enhanced with an increased number of TP scans, suggesting efficient ROS generation of BDP-6 NPs in live cells (Figures 3a and S9).

https://doi.org/10.1021/acs.chemmater.4c00482
Chem. Mater. 2024, 36, 5534−5541

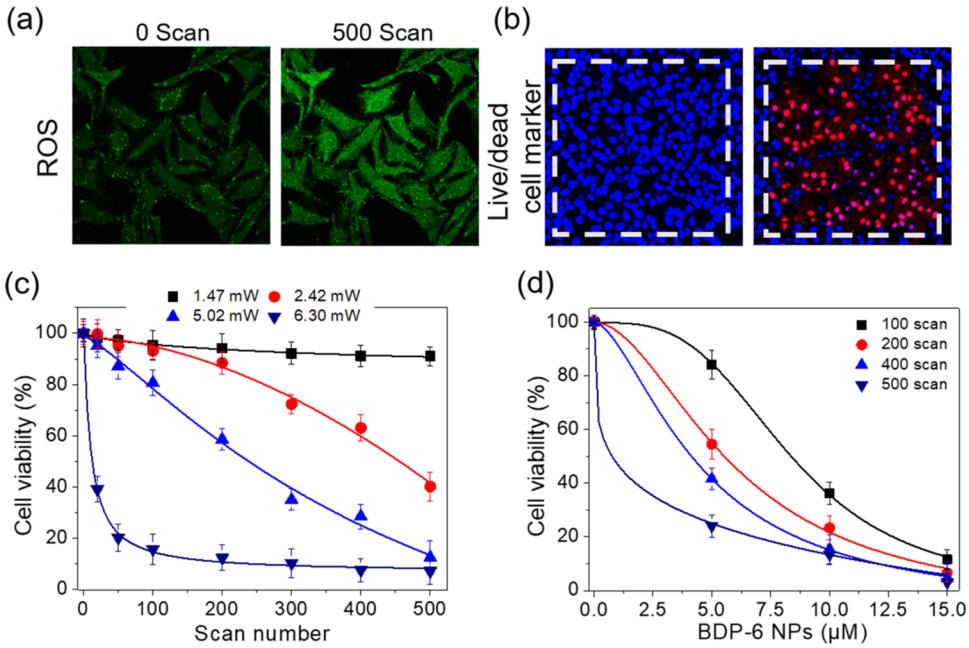

Figure 3. Fluorescence microscopy image of HeLa cells stained with BDP-6 NPs (5 μM) and (a) DCFH-DA (20 μM, ROS probe) or (b) Hoechst 33342/PI as indicators (2/10 μM) followed by TP scans at 5.0 mW laser power. Scale bars = 50 μm. (c) Viability of cells incubated with BDP-6 NPs and irradiated at 780 nm at individual laser powers of 1.5, 2.4, 5.0, and 6.3 mW. (d) Cell viability estimated after 780 nm TP irradiation (6.3 mW).

Encouraged by the above results, TP-induced *in vitro* cellular ablation by the BDP-6 NPs was determined. To count the live/dead cells, we used the Hoechst 33342 and propidium iodide (PI) cell staining method to evaluate TP-PDT efficiency in HeLa cells.[42] HeLa cells were incubated with BDP-6 NPs and Hoechst 33342 for 30 min and irradiated a 290 μm × 290 μm area with a 780 nm TP laser with a 5.02 mW incident power intensity for different scans. We then added PI to the cells and incubated them for 30 min before measuring the dead cell ratio. Figures 3b and S11 show the TP-irradiated region fluorescence from PI (red spots) corresponds to cell death. With increasing numbers of scans, Hoechst 33342 (blue spots) fluorescence decreased and PI-stained cell numbers increased. At 500 TP irradiation scans, BDP-6 NPs-stained cells were completely ablated, whereas the nonirradiated areas showed living Hoechst-stained HeLa cells, indicating TP-induced PDT.

Subsequently, we subjected BDP-6 NPs to LD_{50} measurements at different concentrations and TP laser power (1.47−6.30 mW) to estimate TP-PDT efficiency. TP irradiation at laser power 6.3 mW showed 50% cell death within 15 scans, whereas a similar toxicity level at 2.4 mW took 455 scans (Figure 3c). A clear linear relationship was observed between log (laser power^{-1}) and log (LD_{50}) with 2.76 ± 0.38 linearity gradients (Figure S11c). These results indicate that TP-illuminated cell ablation occurs through a nonlinear PDT process. Furthermore, we investigated IC_{50} under different BDP-6 NP concentrations and an increased number of TP scans (100−500) at 6.3 mW laser power. The IC_{50} values for 100, 200, 400, and 500 scans were 8.3, 5.6, 4.1, and 0.7 μM, respectively (Figure 3d). These confirmed that BDP-6 NPs showed a good PDT effect under TP excitation.

TP-PDT effect in 3D HeLa cell spheroids was investigated by using ROS generation of BDP-6 NPs (Figure 4). To prepare spheroids, HeLa cells were cultured for 48 h in a three-dimensional (3D) cell culture dish. Next, HeLa spheroids were

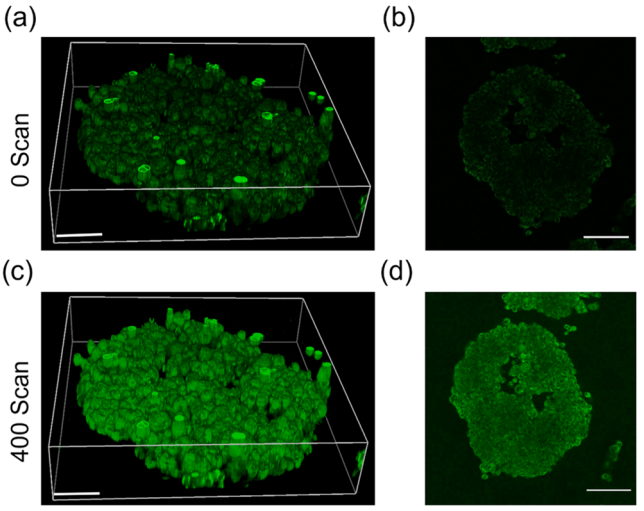

Figure 4. 3D image of HeLa spheroid ROS generation using ROS indicator DHR123. (a, b) 3D images of HeLa spheroids incubated with DHR123 (15 μM) and BDP-6 NPs (100 μM) for 1 h. (c, d) Fluorescence images of HeLa spheroids incubated with DHR123 (15 μM) and BDP-6 NPs (100 μM) after 400 TP irradiation scans. Images were recorded in the 500−550 nm emission window after excitation at 488 nm. Scale bar = 50 μm.

incubated with DHR123 and BDP-6 NPs for 1 h. TP-PDT was conducted by scanning along the Z-Section. Figure 5c,d shows TP excitation at 780 nm after HeLa spheroid BDP-6 NP staining showed bright green DR 123 fluorescence. These results prove that BDP-6 NPs effectively generate ROS in 3D cancer cell models upon TP irradiation.

2.4. In Vivo Imaging and PDT In Vivo. The excellent performance of BDP-6 NPs on cellular imaging and ablation encouraged us to further explore their potential applications in vivo. 4T1 cells (1 × 10^6 cells) were selected and transplanted

https://doi.org/10.1021/acs.chemmater.4c00482
Chem. Mater. 2024, 36, 5534−5541

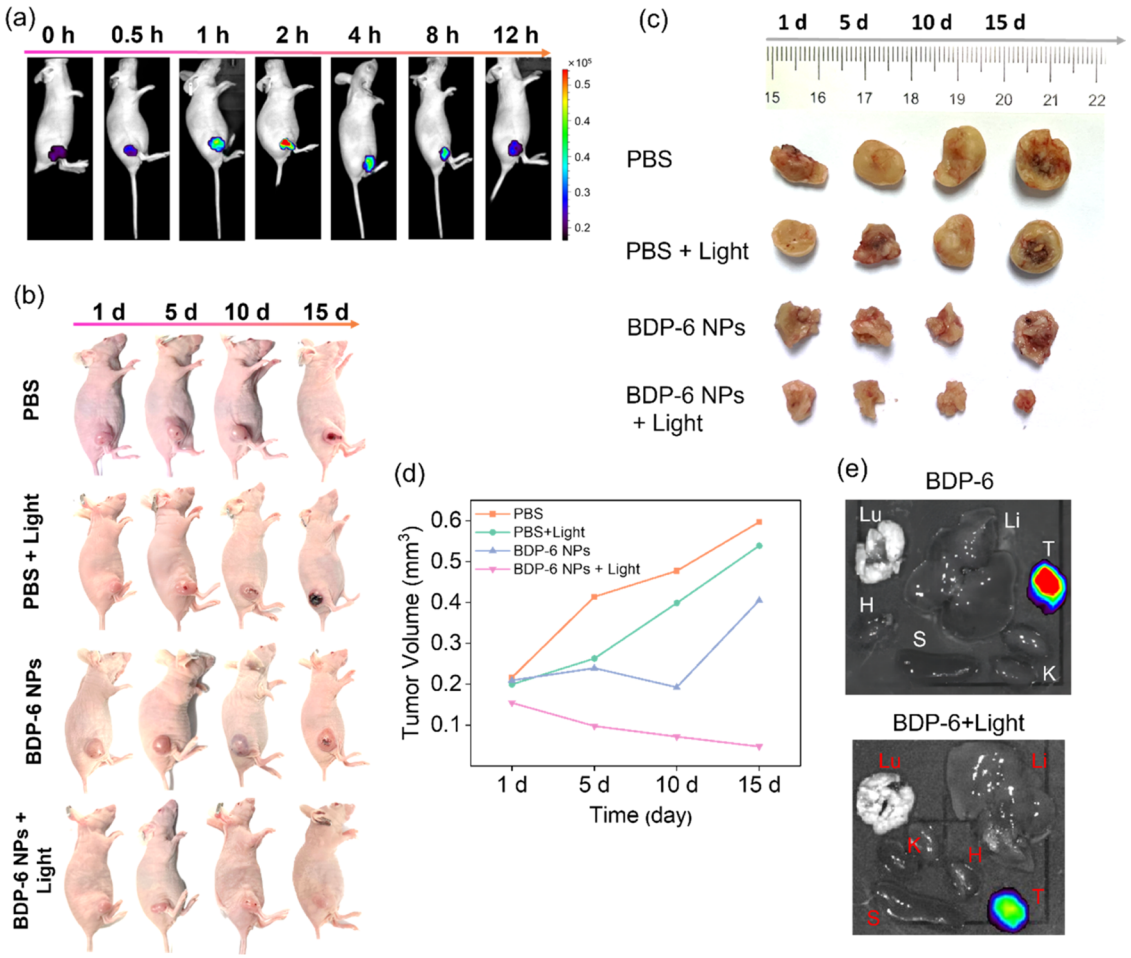

Figure 5. (a) In vivo imaging of BDP-6 NPs (intravenous injection, 10 μM, 100 μL in saline) in female nude BALB/c mice (λ_{ex} = 490 nm, λ_{em} = 500−575 nm) at different time points of 0, 0.5, 1, 2, 4, 8, 12 h. (b) Visualization of BDP-6 NPs in the mouse breast cancer model. Photographs of untreated and PDT-treated mice models (660 nm, 200 mW/cm^2, 15 min) for 1−15 days. The changes in tumor volume and weight. (c) Photographs of untreated and PDT-treated tumors within 15 days. (d) Analysis of tumor volume. (e) 2D ex vivo imaging in separated organs (tumor, heart, liver, spleen, lung, and kidney) sacrificed from mice models.

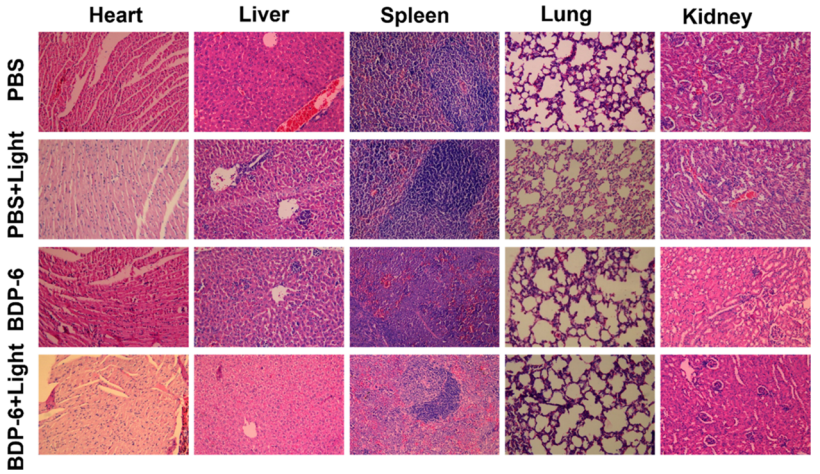

Figure 6. H&E staining of separated organs (heart, liver, spleen, lung, and kidney) sacrificed from untreated and PDT-treated mice models.

subcutaneously into female BALB/c nude mice weighing approximately 20−25 g. After 15 days of inoculation, the mice were injected with BDP-6 NPs via the tail vein during anesthesia. To check the biodistribution of BDP-6 NPs and the optimized incubation time between mice models and the PS, the fluorescence imaging at different time points (0, 0.5, 1, 2, 4, 8, and 12 h) was obtained after intravenous injection of BDP-6 NPs (10 μM, 200 μL in saline) by a living image in vivo imaging system with an excitation of 490 nm and an emission window of 500−575 nm. At 2 h, the fluorescence intensity of

https://doi.org/10.1021/acs.chemmater.4c00482
Chem. Mater. 2024, 36, 5534−5541

the PS reached its maximum level at the tumor sites. Therefore, 2 h was selected as the optimized incubation time.

Venous injection of BDP-6 NPs (10 μM, 200 μL in saline) by a living image in vivo imaging system with an excitation of 490 nm and an emission window of 500−575 nm. At 2 h, the fluorescence intensity of the PS reached its maximum level in the tumor tissues. Therefore, 2 h was selected as the optimized incubation time.

We further investigated the therapeutic efficacy of the PDT treatment using BDP-6 NPs. 4T1 cells were inoculated subcutaneously into mice to construct xenotransplantated tumor mice models, which were then treated with BDP-6 NPs (10 μM, 100 μL in saline) by tail intravenous injection for 1, 5, 10, and 15 days, respectively. The PBS treatment was selected as the control group. The mice models were divided into four groups PBS, PBS + Light, BDP-6, and BDP-6 + Light, respectively, while the corresponding groups without PDT treatment were used as the control groups. Then, the fluorescence images of these mice in four groups were recorded after 2 h tail intravenous injection of BDP-6 NPs and PDT treatment (660 nm, 200 mW/cm^2, 15 min), respectively. As illustrated in Figure 5, the PDT treatment group exhibited excellent tumor inhibition. On the contrary, the fluorescence intensity showed sustainable growth in the control groups.

Before and after PDT treatment, the in vitro tumor volume and weight were recorded within 15 days. After the PDT treatment, the tumor volume and weight decreased. While in the control groups, the tumor volume and weight exhibited sustained growth. 2D in vitro imaging of BDP-6 NPs in various organs (heart, liver, spleen, lungs, and kidneys) and tumors sacrificed in Figure 5 showed that BDP-6 NPs exhibited effective tumor inhibition within 15 days. The successful establishment and PDT efficacy of breast cancer xenotransplanted mouse models were also evaluated and proved by H&E staining (Figure 6).

3. CONCLUSIONS

A novel heavy-atom-free BODIPY PSs (BDP-6) composed of an electron-donating PXZ group and an electron-withdrawing BODIPY core was designed and synthesized for tumor-targeted two-photon photodynamic therapy. The photostable and biocompatible BDP-6 NPs were produced by encapsulating BDP-6 within DSPE-PEG(2000) biotin. Compared to BDP-5 NPs without dimethyl groups, BDP-6 NPs showed brighter emission in the deep red region and more efficient ROS production efficiency under one-photon excitation in aqueous solutions. The BDP-6 NPs could selectively accumulate in cancer cells and effectively kill cancer cells by generating intracellular ROS under green light illumination (one-photon) with low dark toxicity. Interestingly, upon two-photon excitation, the BDP-6 NPs efficiently generated ROS in both aqueous solution and living cells and consequently exhibited excellent 2PE−PDT performance toward cancer cells. In vivo, results demonstrated that BDP-6 NPs showed great potential for tumor-targeted fluorescence imaging and PDT treatment. This work provides a facile, straightforward methodology for developing highly efficient nanophotosensitizers for two-photon excited photodynamic therapy based on heavy-atom-free BODIPY platforms.

4. EXPERIMENTAL SECTION

4.1. Synthesis of 2,6-Dimethyl-4-(10*H*-phenoxazin-10-yl)-benzaldehyde (PXZ-CHO). Phenoxazine (0.5 g, 2.73 mmol), 4-bromo-2,6-dimethylbenzaldehyde (0.64 g, 3.00 mmol), $Pd(OAc)_2$ (0.03 g, 0.14 mmol), *t*-Bu_3PHBF_4 (0.12 g, 0.41 mmol), and K_2CO_3 (1.12 g, 8.10 mmol) were dissolved in toluene (15 mL). The solution was purged with N_2 and stirred at 110 °C for 24 h. Then, the crude product was extracted with DCM (20 mL × 3). The combined organic layers were dried over anhydrous Na_2SO_4 and evaporated the solvent under reduced pressure. The resulting compound was purified by silica gel column chromatography using dichloromethane/hexane (1:1, v/v) as eluent to yield the 2,6-dimethyl-4-(10*H*-phenoxazin-10-yl)benzaldehyde (0.82 g, 95.27%). ^{1}H NMR ($CDCl_3$): δ 10.67 (s, 1H), 7.11 (s, 2H), 6.71−6.59 (m, 6H), 5.98 (d, J = 7.2 Hz, 2H), 2.66 (d, J = 0.8 Hz, 6H). ^{13}C NMR (75 MHz, $CDCl_3$): δ 192.7, 144.4, 144.0, 132.6, 132.3, 131.4, 129.7, 123.3, 121.8, 115.6, 113.4, 20.6.

4.2. Synthesis of BDP-6. 2,6-Dimethyl-4-(10*H*-phenoxazin-10-yl)benzaldehyde (0.5 g, 1.59 mmol) and 2,4-dimethylpyrrole (0.38 g, 3.96 mmol) were dissolved in dry CH_2Cl_2 (40 mL) under a nitrogen atmosphere. One drop of trifluoroacetic acid (TFA) was added, and the mixture was stirred at room temperature for 3 h. After complete aldehyde consumption as monitored by TLC, *p*-chloranil (0.39 g, 1.59 mmol) was added to the reaction mixture. This mixture was stirred for 1 h, and Et_3N (TEA) (3.09 mL, 2.25 g, 22.20 mmol) was added. After 30 min, $BF_3{\cdot}OEt_2$ (2.74 mL, 3.15 g, 22.20 mmol) was slowly added to the mixture. Then, the solvent was removed under reduced pressure. The resulting compound was purified by silica gel column chromatography using dichloromethane/hexane (3:2, v/v) as eluent to yield pure BDP-6 (0.64 g, 76%). ^{1}H NMR ($CDCl_3$): δ 7.16 (s, 2H), 6.72−6.58 (m, 6H), 6.04 (s, 2H), 5.91 (dd, J = 7.7, 1.6 Hz, 2H), 2.59 (s, 6H), 2.23 (s, 6H), 1.55 (s, 6H). ^{13}C NMR (75 MHz, $CDCl_3$): δ 155.9, 141.6, 139.8, 139.1, 134.7, 130.1, 123.2, 121.3, 112.9, 19.7, 14.7, 13.5. ESI-MS calcd. for $C_{33}H_{31}BF_2N_3O$ $[M + H]^+$: 534.2528, found: 534.2533.

4.3. Preparation of BDP-5/BDP-6 Nanoparticles (BDP-5/BDP-6 NPs). BDP-5/BDP-6 (1.0 mg) and 1,2-distearoyl-*sn*-glycero-3-phosphoethanolamine-*N*-[biotinyl(poly(ethylene glycol))-2000] (DSPE-PEG(2000) biotin, 5 mg) were dissolved in 1 mL of tetrahydrofuran (THF). The organic mixture was added dropwise to 10 mL of deionized water (DW). The solution was stirred overnight to ensure THF evaporation. Then, the solution was filtered through a 0.20 μm disposable membrane to obtain a filtered BDP-5/BDP-6 NPs solution. After 30 min centrifugation, the supernatant was removed with a pipet. 200 μL of DW was added to the remaining precipitate for further use.

■ ASSOCIATED CONTENT

Supporting Information

The Supporting Information is available free of charge at https://pubs.acs.org/doi/10.1021/acs.chemmater.4c00482.

Experimental data; synthesis, nanoparticle preparation, and photophysical measurements; ^{1}H and ^{13}C NMR spectra of all compounds; in vitro and in vivo studies of BDP-6 NPs; UV−vis absorption and PL spectra; and fluorescent images (PDF)

■ AUTHOR INFORMATION

Corresponding Authors

Rui Wang − *Key Laboratory of Hainan Trauma and Disaster Rescue, The First Affiliated Hospital of Hainan Medical University, Hainan Medical University, Haikou 571199, China*; Email: wangrui@hainmc.edu.cn

Hwan Myung Kim − *Department of Chemistry and Energy Systems Research, Ajou University, Suwon 16499, Korea*; orcid.org/0000-0002-4112-9009; Email: kimhm@ajou.ac.kr

https://doi.org/10.1021/acs.chemmater.4c00482
Chem. Mater. 2024, 36, 5534−5541

Fabiao Yu − *Key Laboratory of Hainan Trauma and Disaster Rescue, The First Affiliated Hospital of Hainan Medical University, Hainan Medical University, Haikou 571199, China;* orcid.org/0000-0003-0073-6299; Email: yufabiao@hainmc.edu.cn

Juyoung Yoon − *Department of Chemistry and Nanoscience, Ewha Womans University, Seoul 03760, Republic of Korea;* orcid.org/0000-0002-1728-3970; Email: jyoon@ewha.ac.kr

Authors

Van-Nghia Nguyen − *Department of Chemistry and Nanoscience, Ewha Womans University, Seoul 03760, Republic of Korea; School of Chemistry and Life Sciences, Hanoi University of Science and Technology, Hanoi 100000, Vietnam;* orcid.org/0000-0001-6553-8176

Dong Joon Lee − *Department of Chemistry and Energy Systems Research, Ajou University, Suwon 16499, Korea*

Dianqi Zhang − *Key Laboratory of Hainan Trauma and Disaster Rescue, The First Affiliated Hospital of Hainan Medical University, Hainan Medical University, Haikou 571199, China*

Jeongsun Ha − *Department of Chemistry and Nanoscience, Ewha Womans University, Seoul 03760, Republic of Korea*

Kunemadihalli Mathada Kotraiah Swamy − *Department of Chemistry and Nanoscience, Ewha Womans University, Seoul 03760, Republic of Korea*

Complete contact information is available at: https://pubs.acs.org/10.1021/acs.chemmater.4c00482

Author Contributions

[⊥]V.-N.N., D.J.L., D.Z., and J.H. authors contributed equally to this study.

Notes

The authors declare no competing financial interest.

■ ACKNOWLEDGMENTS

This study was supported by grants from the National Research Foundation of Korea (NRF) funded by the Korean government (MSIP) (no. 2022R1I1A1A01055905 for V.-N.N., no. 2022R1A2B5B03001607 for H.M.K., and RS-2023-00217701 for J.Y.). K.M.K.S. acknowledges the support of the Brain Pool program funded by the Ministry of Science and ICT through the National Research Foundation of Korea (2022H1D3A2A01096309). This work was also supported by the National Natural Science Foundation of China (no. 22264013), Hainan Province Clinical Medical Center (2021), Project for Functional Materials and Molecular Imaging Science Innovation Group of Hainan Medical University. High-resolution mass spectrometer analysis was performed on the Synapt G2-HDMS mass spectrometer (Waters, Manchester, U.K.), which was operated on the MassLynx 4.1 software at KBSI (Korea Basic Science Institute, Ochang, Center of Research Equipment).

■ REFERENCES

(1) Lucky, S. S.; Soo, K. C.; Zhang, Y. Nanoparticles in photodynamic therapy. *Chem. Rev.* **2015**, *115* (4), 1990−2042.

(2) Celli, J. P.; Spring, B. Q.; Rizvi, I.; Evans, C. L.; Samkoe, K. S.; Verma, S.; Pogue, B. W.; Hasan, T. Imaging, and photodynamic therapy: mechanisms, monitoring, and optimization. *Chem. Rev.* **2010**, *110* (5), 2795−2838.

(3) Wang, S.; Wu, W.; Manghnani, P.; Xu, S.; Wang, Y.; Goh, C. C.; Ng, L. G.; Liu, B. Polymerization-Enhanced Two-Photon Photosensitization for Precise Photodynamic Therapy. *ACS Nano* **2019**, *13* (3), 3095−3105.

(4) Jung, H. S.; Han, J.; Shi, H.; Koo, S.; Singh, H.; Kim, H. J.; Sessler, J. L.; Lee, J. Y.; Kim, J. H.; Kim, J. S. Overcoming the Limits of Hypoxia in Photodynamic Therapy: A Carbonic Anhydrase IX-Targeted Approach. *J. Am. Chem. Soc.* **2017**, *139* (22), 7595−7602.

(5) Nguyen, V.-N.; Qi, S.; Kim, S.; Kwon, N.; Kim, G.; Yim, Y.; Park, S.; Yoon, J. An Emerging Molecular Design Approach to Heavy-Atom-Free Photosensitizers for Enhanced Photodynamic Therapy under Hypoxia. *J. Am. Chem. Soc.* **2019**, *141* (41), 16243−16248.

(6) Nguyen, V.-N.; Yan, Y.; Zhao, J.; Yoon, J. Heavy-Atom-Free Photosensitizers: From Molecular Design to Applications in the Photodynamic Therapy of Cancer. *Acc. Chem. Res.* **2021**, *54* (1), 207−220.

(7) Li, M.; Xiong, T.; Du, J.; Tian, R.; Xiao, M.; Guo, L.; Long, S.; Fan, J.; Sun, W.; Shao, K.; Song, X.; Foley, J. W.; Peng, X. Superoxide Radical Photogenerator with Amplification Effect: Surmounting the Achilles' Heels of Photodynamic Oncotherapy. *J. Am. Chem. Soc.* **2019**, *141* (6), 2695−2702.

(8) Zhao, X.; Liu, J.; Fan, J.; Chao, H.; Peng, X. Recent progress in photosensitizers for overcoming the challenges of photodynamic therapy: from molecular design to application. *Chem. Soc. Rev.* **2021**, *50* (6), 4185−4219.

(9) Zhou, J.; Rao, L.; Yu, G.; Cook, T. R.; Chen, X.; Huang, F. Supramolecular cancer nanotheranostics. *Chem. Soc. Rev.* **2021**, *50* (4), 2839−2891.

(10) Wang, D.; Lee, M. M. S.; Shan, G.; Kwok, R. T. K.; Lam, J. W. Y.; Su, H.; Cai, Y.; Tang, B. Z. Highly Efficient Photosensitizers with Far-Red/Near-Infrared Aggregation-Induced Emission for In Vitro and In Vivo Cancer Theranostics. *Adv. Mater.* **2018**, *30* (39), No. 1802105.

(11) Qi, S.; Kwon, N.; Yim, Y.; Nguyen, V.-N.; Yoon, J. Fine-tuning the electronic structure of heavy-atom-free BODIPY photosensitizers for fluorescence imaging and mitochondria-targeted photodynamic therapy. *Chem. Sci.* **2020**, *11* (25), 6479−6484.

(12) Liu, S.; Feng, G.; Tang, B. Z.; Liu, B. Recent advances of AIE light-up probes for photodynamic therapy. *Chem. Sci.* **2021**, *12* (19), 6488−6506.

(13) Zhang, J. J.; Ning, L. L.; Huang, J. G.; Zhang, C.; Pu, K. Y. Activatable molecular agents for cancer theranostics. *Chem. Sci.* **2020**, *11* (3), 618−630.

(14) Feng, G.; Zhang, G. Q.; Ding, D. Design of superior phototheranostic agents guided by Jablonski diagrams. *Chem. Soc. Rev.* **2020**, *49* (22), 8179−8234.

(15) Li, X.; Kim, C. Y.; Lee, S.; Lee, D.; Chung, H. M.; Kim, G.; Heo, S. H.; Kim, C.; Hong, K. S.; Yoon, J. Nanostructured Phthalocyanine Assemblies with Protein-Driven Switchable Photoactivities for Biophotonic Imaging and Therapy. *J. Am. Chem. Soc.* **2017**, *139* (31), 10880−10886.

(16) Huynh, E.; Zheng, G. Engineering multifunctional nanoparticles: all-in-one versus one-for-all. *Wiley Interdiscip. Rev.: Nanomed. Nanobiotechnol.* **2013**, *5* (3), 250−265, DOI: 10.1002/wnan.1217.

(17) Li, X.; Lee, S.; Yoon, J. Supramolecular photosensitizers rejuvenate photodynamic therapy. *Chem. Soc. Rev.* **2018**, *47* (4), 1174−1188.

(18) Shen, Y.; Shuhendler, A. J.; Ye, D.; Xu, J. J.; Chen, H. Y. Two-photon excitation nanoparticles for photodynamic therapy. *Chem. Soc. Rev.* **2016**, *45* (24), 6725−6741.

(19) Han, R.; Zhao, M.; Wang, Z.; Liu, H.; Zhu, S.; Huang, L.; Wang, Y.; Wang, L.; Hong, Y.; Sha, Y.; Jiang, Y. Super-efficient in Vivo Two-Photon Photodynamic Therapy with a Gold Nanocluster as a Type I Photosensitizer. *ACS Nano* **2020**, *14* (8), 9532−9544.

(20) Nguyen, V.-N.; Park, S. J.; Qi, S.; Ha, J.; Heo, S.; Yim, Y.; Baek, G.; Lim, C. S.; Lee, D. J.; Kim, H. M.; Yoon, J. Design and synthesis of efficient heavy-atom-free photosensitizers for photodynamic therapy of cancer. *Chem. Commun.* **2020**, *56* (77), 11489−11492.

(21) Gu, B.; Wu, W. B.; Xu, G. X.; Feng, G. X.; Yin, F.; Chong, P. H. J.; Qu, J. L.; Yong, K. T.; Liu, B. Precise Two-Photon Photodynamic Therapy using an Efficient Photosensitizer with Aggregation-Induced Emission Characteristics. *Adv. Mater.* **2017**, *29* (28), No. 1701076.
(22) Sun, Z. Y.; Zhang, L. P.; Wu, F. P.; Zhao, Y. X. Photosensitizers for Two-Photon Excited Photodynamic Therapy. *Adv. Funct. Mater.* **2017**, *27* (48), No. 1704079.
(23) Qin, Y.; Liu, X.; Jia, P. P.; Xu, L.; Yang, H. B. BODIPY-based macrocycles. *Chem. Soc. Rev.* **2020**, *49*, 5678−5703.
(24) Shi, Z.; Han, X.; Hu, W.; Bai, H.; Peng, B.; Ji, L.; Fan, Q.; Li, L.; Huang, W. Bioapplications of small molecule Aza-BODIPY: from rational structural design to in vivo investigations. *Chem. Soc. Rev.* **2020**, *49* (21), 7533−7567.
(25) Nguyen, V.-N.; Ha, J.; Cho, M.; Li, H.; Swamy, K.; Yoon, J. Recent developments of BODIPY-based colorimetric and fluorescent probes for the detection of reactive oxygen/nitrogen species and cancer diagnosis. *Coord. Chem. Rev.* **2021**, *439*, No. 213936.
(26) Cheng, M. H. Y.; Harmatys, K. M.; Charron, D. M.; Chen, J.; Zheng, G. Stable J-Aggregation of an aza-BODIPY-Lipid in a Liposome for Optical Cancer Imaging. *Angew. Chem., Int. Ed.* **2019**, *58* (38), 13394−13399.
(27) Zhao, J.; Wu, W.; Sun, J.; Guo, S. Triplet photosensitizers: from molecular design to applications. *Chem. Soc. Rev.* **2013**, *42* (12), 5323−5351.
(28) Kamkaew, A.; Lim, S. H.; Lee, H. B.; Kiew, L. V.; Chung, L. Y.; Burgess, K. BODIPY dyes in photodynamic therapy. *Chem. Soc. Rev.* **2013**, *42* (1), 77−88.
(29) Yogo, T.; Urano, Y.; Ishitsuka, Y.; Maniwa, F.; Nagano, T. Highly efficient and photostable photosensitizer based on BODIPY chromophore. *J. Am. Chem. Soc.* **2005**, *127* (35), 12162−12163.
(30) Linden, G.; Zhang, L.; Pieck, F.; Linne, U.; Kosenkov, D.; Tonner, R.; Vazquez, O. Conditional Singlet Oxygen Generation through a Bioorthogonal DNA-targeted Tetrazine Reaction. *Angew. Chem., Int. Ed.* **2019**, *58* (37), 12868−12873.
(31) Won, M.; Koo, S.; Li, H.; Sessler, J. L.; Lee, J. Y.; Sharma, A.; Kim, J. S. An Ethacrynic Acid-Brominated BODIPY Photosensitizer (EA-BPS) Construct Enhances the Lethality of Reactive Oxygen Species in Hypoxic Tumor-Targeted Photodynamic Therapy. *Angew. Chem., Int. Ed.* **2021**, *60* (6), 3196−3204.
(32) Cakmak, Y.; Kolemen, S.; Duman, S.; Dede, Y.; Dolen, Y.; Kilic, B.; Kostereli, Z.; Yildirim, L. T.; Dogan, A. L.; Guc, D.; Akkaya, E. U. Designing excited states: theory-guided access to efficient photosensitizers for photodynamic action. *Angew. Chem., Int. Ed.* **2011**, *50* (50), 11937−11941.
(33) Wang, Z.; Huang, L.; Yan, Y.; El-Zohry, A. M.; Toffoletti, A.; Zhao, J.; Barbon, A.; Dick, B.; Mohammed, O. F.; Han, G. Elucidation of the Intersystem Crossing Mechanism in a Helical BODIPY for Low-Dose Photodynamic Therapy. *Angew. Chem., Int. Ed.* **2020**, *59* (37), 16114−16121.
(34) Nguyen, V.-N.; Yim, Y.; Kim, S.; Ryu, B.; Swamy, K. M. K.; Kim, G.; Kwon, N.; Kim, C. Y.; Park, S.; Yoon, J. Molecular Design of Highly Efficient Heavy-Atom-Free Triplet BODIPY Derivatives for Photodynamic Therapy and Bioimaging. *Angew. Chem., Int. Ed.* **2020**, *59* (23), 8957−8962.
(35) Awuah, S. G.; You, Y. Boron dipyrromethene (BODIPY)-based photosensitizers for photodynamic therapy. *RSC Adv.* **2012**, *2* (30), 11169−11183.
(36) Kue, C. S.; Ng, S. Y.; Voon, S. H.; Kamkaew, A.; Chung, L. Y.; Kiew, L. V.; Lee, H. B. Recent strategies to improve boron dipyrromethene (BODIPY) for photodynamic cancer therapy: an updated review. *Photochem. Photobiol. Sci.* **2018**, *17* (11), 1691−1708.
(37) Prieto-Montero, R.; Prieto-Castaneda, A.; Sola-Llano, R.; Agarrabeitia, A. R.; Garcia-Fresnadillo, D.; Lopez-Arbeloa, I.; Villanueva, A.; Ortiz, M. J.; de la Moya, S.; Martinez-Martinez, V. Exploring BODIPY Derivatives as Singlet Oxygen Photosensitizers for PDT. *Photochem. Photobiol.* **2020**, *96* (3), 458−477.
(38) Sztandera, K.; Gorzkiewicz, M.; Klajnert-Maculewicz, B. Nanocarriers in photodynamic therapy-in vitro and in vivo studies. *Wiley Interdiscip. Rev.: Nanomed. Nanobiotechnol.* **2020**, *12* (3), 1509 DOI: 10.1002/wnan.1599.
(39) Li, K.; Liu, B. Polymer-encapsulated organic nanoparticles for fluorescence and photoacoustic imaging. *Chem. Soc. Rev.* **2014**, *43* (18), 6570−6597.
(40) Kolemen, S.; Akkaya, E. U. Reaction-based BODIPY probes for selective bio-imaging. *Coord. Chem. Rev.* **2018**, *354*, 121−134.
(41) Ren, W. X.; Han, J.; Uhm, S.; Jang, Y. J.; Kang, C.; Kim, J. H.; Kim, J. S. Recent development of biotin conjugation in biological imaging, sensing, and target delivery. *Chem. Commun.* **2015**, *51* (52), 10403−10418.
(42) Juvekar, V.; Lim, C. S.; Lee, D. J.; Park, S. J.; Song, G. O.; Kang, H.; Kim, H. M. An azo dye for photodynamic therapy that is activated selectively by two-photon excitation. *Chem. Sci.* **2021**, *12* (1), 427−434.

https://doi.org/10.1021/acs.chemmater.4c00482
Chem. Mater. 2024, 36, 5534−5541